Bioorganic & Medicinal Chemistry 16 (2008) 8349–8358

Contents lists available at ScienceDirect

Bioorganic & Medicinal Chemistry

journal homepage: www.elsevier.com/locate/bmc

CYP19 (aromatase): Exploring the scaffold flexibility for novel selective inhibitors

Sabrina Castellano [a,*], Giorgio Stefancich [b], Rino Ragno [c,*], Katarzyna Schewe [d], Marisabella Santoriello [a], Antonia Caroli [c], Rolf W. Hartmann [d], Gianluca Sbardella [a]

[a] Dipartimento di Scienze Farmaceutiche, Università di Salerno, Via Ponte Don Melillo, I-84084 Fisciano (SA), Italy
[b] Dipartimento di Scienze Farmaceutiche, Università di Trieste, P.le Europa 1, I-34127 Trieste, Italy
[c] Dipartimento di Chimica e Tecnologie del Farmaco, Università degli studi di Roma 'La Sapienza', P.le Aldo Moro 5, I-00185 Roma, Italy
[d] Pharmaceutical and Medicinal Chemistry, Saarland University, PO Box 151150, D-66041 Saarbrücken, Germany

ARTICLE INFO

Article history:
Received 20 May 2008
Revised 9 August 2008
Accepted 22 August 2008
Available online 26 August 2008

Keywords:
Aromatase inhibitors
CYP19
3D-QSAR
Ligand-based drug design
Antifungal agents

ABSTRACT

Several derivatives out of a series of antifungal agents exhibited a good inhibitory potency against aromatase as well as a fairly good selectivity toward CYP17, even if lacking H-bond accepting substituents. Their common structural feature is a flexible backbone that did not fit into previously reported CYP19 models. Thus, a ligand-based approach was exploited to develop a novel statistically robust, self-consistent and predictive 3D-QSAR model herein proposed as a helpful tool to design new aromatase inhibitors.

1. Introduction

Estrogen-dependent (ER^+) breast cancer accounts for approximately one-third of all breast cancer patients, and two-thirds of cases of postmenopausal breast cancer.[1,2] This tumor contains estrogen receptors and requires estrogens for tumor growth and indeed estrogens are maintained in postmenopausal women breast tissue nearly at the same level as in premenopausal women.[3]

Aromatase is a cytochrome P450 (CYP19; EC 1.14.14.1) enzyme that catalyzes the conversion of androgens androstenedione and testosterone to the aromatic estrogenic steroids estrone and estradiol, respectively, through the aromatization of the A ring of the substrate.[4] This enzyme is present in breast tissue and is an important pharmacological target in the anti-cancer therapy, because intratumoral aromatase is the source of local estrogen production in breast cancer tissues.[5] As a matter of fact, suppression of estrogen biosynthesis by aromatase inhibition represents an effective approach for the treatment of hormone-sensitive breast cancer and several classes of steroidal and nonsteroidal AR inhibitors (AIs), such as aminoglutethimide and imidazole or triazole derivatives (Fig. 1), were actually developed in the last two decades.[6–25] Among the latter, the recently FDA-approved anastrozole[26] and letrozole,[27] as well as the steroid exemestane,[28] are widely used, even as the first-line drugs in the therapy of breast cancer.[29,30] However, the occurrence of important side effects associated with the prolonged clinical use of AIs[31,32] calls for the search of new, potent, more selective, and less toxic CYP19 inhibitors.

One of the most important feature for strong inhibitor binding to CYP enzymes is the capability to interact as the sixth ligand with the iron atom of the heme group, always present in this enzyme family. This coordination is excellently performed by the lone pair carried on the sp^2 hybridized imidazole nitrogen but other electron rich heterocycles might be accepted in this position as well. Therefore we were rather surprised that the introduction of 1-amino-azoles was little studied in the development of AIs, particularly if considering the high potency and selectivity of compound YM-511 (Fig. 1),[16,25] the most known among the derivatives containing this moiety.

During our search for novel antifungal agents, we previously reported the synthesis of a large number of compounds,[33–36] many of which were characterized by the presence of a common scaffold containing a central 1-amino-azole moiety and two aromatic portions separated from the central one by methylenic linkers (Fig. 2). As the pursuing of new entities possessing aromatase inhibitory properties is still active, we decided to firstly explore the potential

* Corresponding authors. Tel.: +39 089 96 9244; fax: +39 089 96 9602 (S.C.); tel.: +39 06 4991 3937; fax: +39 06 491 491 (R.R.).
E-mail addresses: scastellano@unisa.it (S. Castellano), rino.ragno@uniroma1.it (R. Ragno).

0968-0896/$ - see front matter © 2008 Elsevier Ltd. All rights reserved.
doi:10.1016/j.bmc.2008.08.046

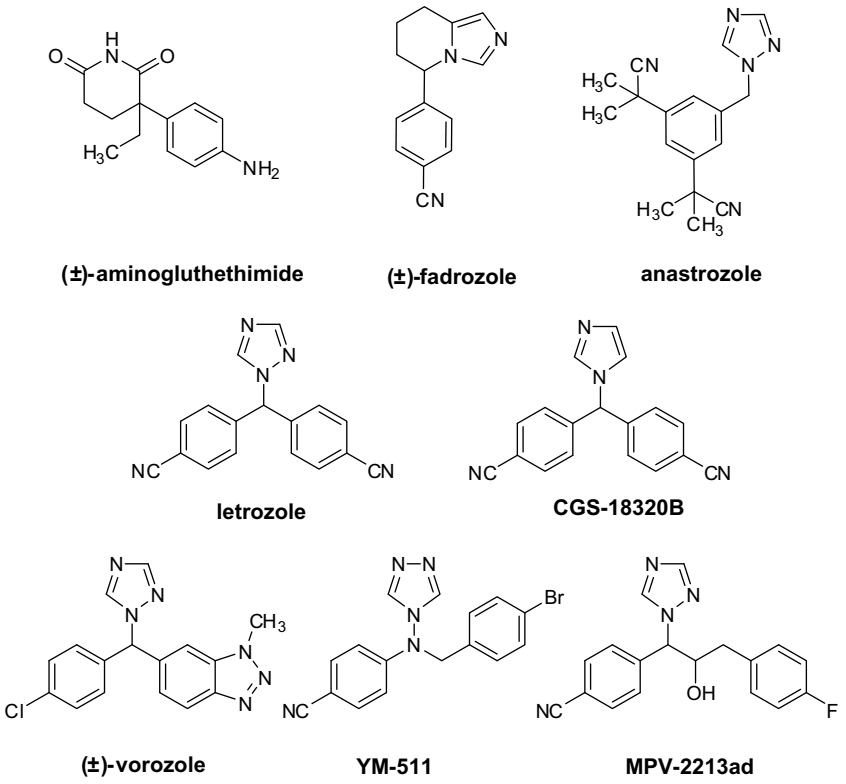

Figure 1. Nonsteroidal aromatase inhibitors.

of this template, before decorating it with hydrogen bond acceptors at an appropriate distance from the heterocycle, credited to provide auxiliary interactions that could further improve the binding affinity and the potency of the inhibitors.[21,37–39]

Therefore, we tested the in vitro inhibiting activity of derivatives **1–4** (Fig. 2) against aromatase and against 17α-hydroxylase/17,20-lyase (CYP17), another cytochrome P450 involved in the synthesis of androgens, to evaluate their selectivity toward a related enzyme. The in vitro assays evidenced a very good inhibitory activity against aromatase for a few tested derivatives. Unexpectedly, we were able to obtain (vide infra) only a poor correlation between the activities of these compounds and their fitting into the models precedently described by other groups in collaboration with one of us (R.W.H.).[20–24,40–43]

For this reason we herein describe the building of a novel robust and more versatile 3D-QSAR model and the validation of its ability to predict the aromatase inhibiting activity of a set of newly synthesized derivatives (Fig. 3).

2. Results and discussion

2.1. Chemistry

The novel derivatives **1bq**, **1eq**, **1nq**, **1er**, **1nr**, **2bq**, and **2eq** were prepared (Schemes 1 and 2) following the same synthetical route previously reported by us.[33–36]

Briefly, the 1-aminoimidazole derivatives **1** were prepared starting from the Schiff bases **5b**, **5e,** and **5n**, synthesized by adding imidazole to a neutral solution of hydroxylamine-*O*-sulfonic acid in water and then treating the crude residue obtained after acidification and elimination of the water with a solution of the proper aromatic aldehyde in ethanol.[34] The reduction of the Schiff bases with sodium borohydride in methanol yielded the corresponding secondary amines **6b**, **6e,** and **6n** which were finally alkylated with 2- chloro-5-(chloromethyl)thiophene or with 7-(bromomethyl)-benzothiophene[47] in the presence of tetrabutylammonium hydrogen sulfate in dichloromethane/50% sodium hydroxide aqueous solution to furnish derivatives **1bq**, **1eq**, **1nq**, and **1nr**. The alkylation of the amine **6n** with 7-(bromomethyl)benzothiophene was accomplished only in the presence of potassium *tert*-butoxide and 18-crown-6 in diethyl ether to obtain the final compound **1er** (Scheme 1).[35]

Derivatives **2bq** and **2eq** were in turn prepared by alkylation of the imidazolylacetophenones **7b**[48] and **7e**[49] with 2-chloro-5-(chloromethyl)thiophene in THF in the presence of sodium hydride to give the intermediate ketones **8bq** and **8eq** which were reduced following the Huang–Minlon modification of the Wolff–Kishner reaction[36] to yield the final derivatives **2bq** and **2eq** (Scheme 2).

2.2. Biological assays

Compounds **1–4** were tested for inhibition of aromatase using human placental microsomes incubated with 1β[^{3}H]androstenedione and measuring the tritiated water formed during the aromatization of the substrate, as previously described.[44] For the CYP17 inhibition tests, human CYP17 expressed in *Escherichia coli,* P450 reductase and progesterone as substrate were used.[45] The IC_{50} value of fadrozole tested in our test system[46] is also reported for comparison (Table 1).

Interestingly, even if lacking H-bond accepting substituents as CN or NO_2,[21,37–39] several among the tested derivatives exhibited a good inhibitory potency against aromatase (compare, e.g., IC_{50} values of compounds **1bk** and **2bk** with that of the reference compound fadrozole) as well as a fairly good selectivity toward CYP17. As a general rule imidazole-containing derivatives resulted more active than the triazole (both symmetrical 1,3,4 and asymmetrical 1,2,4) counterparts (compare IC_{50} values of compounds **1bd** and **1bn** with those of compounds **3bd**, **3bn** and **4bd** and **4bn**, respec-

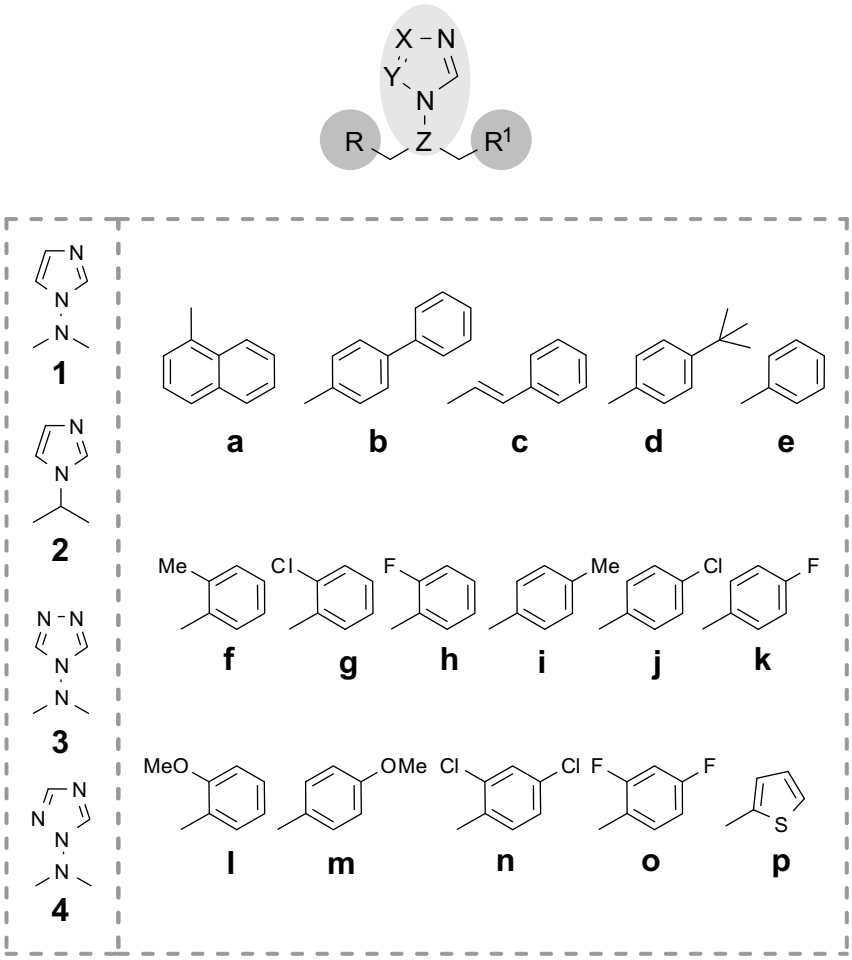

Figure 2. Antifungal compounds **1**–**4** tested as aromatase inhibitors. In the numeration of the compounds the number (**1**–**4**) indicates the azole moiety while the two letters (**a**–**p**) specify the combination of aromatic moieties R and R^1. The various alternatives for X, Y, and Z are as shown in structures **1**–**4**.

tively). As far as the aromatic moieties (R and R^1, Fig. 2) are concerned, in agreement with what was recently reported by Potter and co-workers[39] the introduction of a biphenyl system as **R** substituent (Fig. 2) was beneficial for the activity of the compounds while the 1-naphthyl-substituted derivatives resulted less active (compare IC_{50} values of compounds **1ad** and **1an** with those of **2bd** and **2bn**, respectively). Nevertheless, the replacement of the biphenyl group with a 4-*tert*-butylphenyl further improved the efficacy of the derivatives, even if a decrease in selectivity was also observed (compare IC_{50} values of compounds **1bn** and **1dn**). As regards to the R^1 substituent (Fig. 2), the effects of the introduction of 2- or 4-substituted phenyl rings seemed to correlate with the electronegativity of the substituents (F > Cl > H), that is, with the ability of the latter to act as H-bond acceptors, particularly if in the *para*-position of the benzene ring. In fact, 4-fluorophenyl derivatives **1bk** and **2bk** were the most active among all tested compounds, being only 3.7- and 2.2-fold less active than fadrozole, respectively (Table 1). Moreover, sterical hindrance appeared to be detrimental for the activity (compare, e.g., IC_{50} values of compounds **1be**, **1bi,** and **1bd**). Interestingly, the replacement of the substituted benzene with a thiophene ring resulted in an enhancement of both the inhibitory potency and the selectivity toward CYP17 (compare IC_{50} values of compounds **1dn** and **1dp**).

The presence of the nitrogen atom directly linked to the N_1 of the azole moiety did not significantly influenced the inhibiting capability of tested molecules. In fact, the activities of derivatives **1** were comparable or slightly inferior to those of derivatives **2**, with the exception of 2-halo-substituted compounds which resulted threefold more active in the 1-amino-imidazole series **1** (compare IC_{50} values of compounds **1bg** and **1bh** with those of compounds **2bg** and **2bh**, respectively).

2.3. 3D-QSAR studies

In order to gain further insight, a three-dimensional quantitative structure–activity relationship (3D-QSAR) model was then developed using a training set with a large structural variety containing derivatives **1–2** and **4ac**, **4cn**, **4dc,** and **4dp**[50] (31 compounds) plus additional 90 compounds (Supplementary data) previously reported as aromatase inhibitors.[20–22,40–43,51] It is worth mentioning that, to avoid any lack of homogeneity in the biological data, all the selected compounds had been tested in our laboratory and following the same experimental protocol.

The structures were built using the standalone version of the program PRODRG2.[52–54] Due to the lack of any structural information we tried to perform a structure-based alignment using a CYP19 homology model developed by Favia et al. (pdb entry code 1tqa).[55] Nevertheless any attempt to build a statistically significant 3D-QSAR model failed, maybe due to the lack of the correct Fe parameters and also to the fact that in the aforementioned paper by Favia et al. only the aromatase minimized average structure of the molecular dynamics studies was available. Therefore we turned to develop a ligand-based alignment by means of the program Surflex developed by Jain.[56] For the flexible Surflex-based

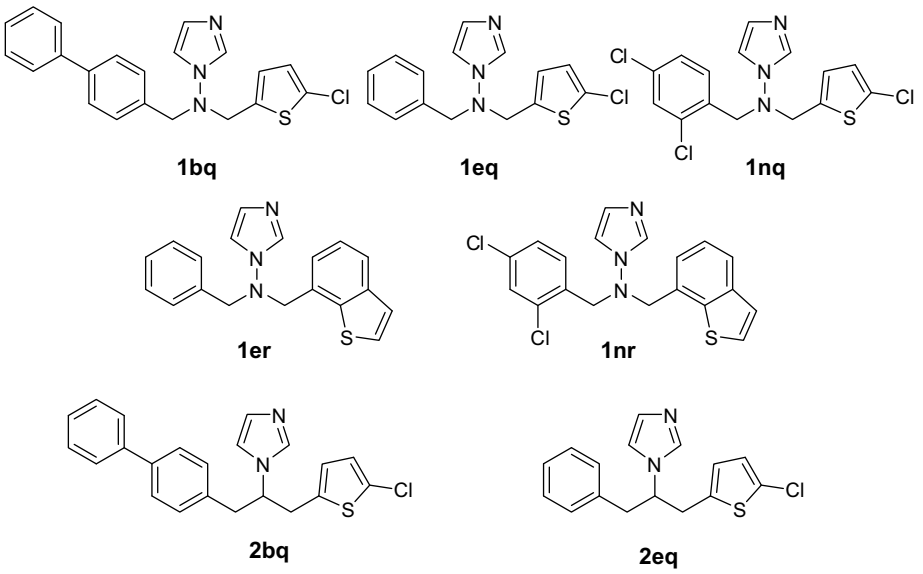

Figure 3. Newly synthesized compounds used to test the predictive ability of the 3D-QSAR model described in the paper.

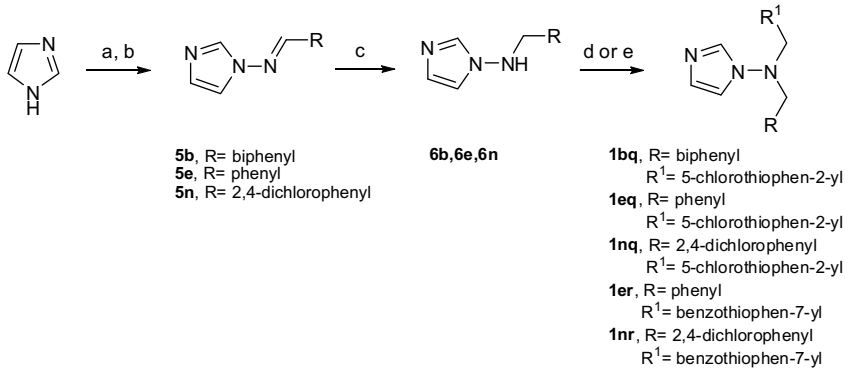

Scheme 1. Reagents and conditions: (a) NH_2OSO_3H, water, $NaHCO_3$; (b) biphenyl-4-carbaldehyde or benzaldehyde or 2,4-dichlorobenzaldehyde, ethanol, HCl; (c) NaBH4, methanol; (d) 2-chloro-5-(chloromethyl)thiophene or 7-(bromomethyl)benzothiophene, 50% aq NaOH, TBAHS, dichloromethane; (e) 7-(bromomethyl) benzothiophene, ^{t}BuOK, 18-C-6, diethyl ether.

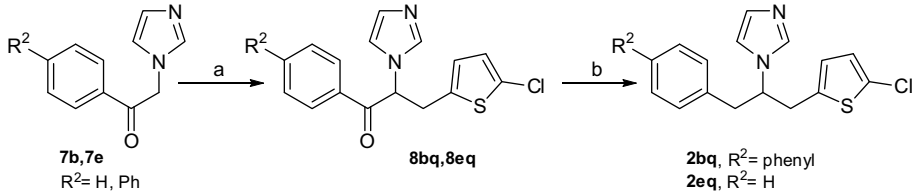

Scheme 2. Reagents and conditions: (a) 2-chloro-5-(chloromethyl)thiophene, NaH, THF, 50 °C; (b) hydrazine hydrate, KOH, diethyleneglycol, 190 °C.

alignment (Fig. 4) the crystal structures of the three highly active aromatase inhibitors CGS-18320B,[57] fadrozole,[57] and vorozole[58] (Fig. 1) were used as reference molecules (Supplementary data).

Once the structures were aligned, a GRID/GOLPE[59] procedure was applied to build the 3D-QSAR model. To this purpose, the water, DRY, OH and C=GRID probes alone and combinations of them (DRY+OH and DRY+water) were tried and only the preliminary GRID/GOLPE models showing the higher q^2 values were refined by sequential fractional factorial design (FFD) selections. The DRY+OH combination gave the best statistical results (Table 2). Furthermore since many of the molecules included in the training set contained a chiral center, two models were initially built: one including only compounds with *R*-configuration (*R*-model) and the second containing only derivatives with *S*-absolute configurations (*S*-model). Achiral compounds were equally added to both models. Yet, the statistical results obtained by the use of different probes for each model were in favor of the *R*-model derived with DRY+OH probes combination, thus we decided to discard the *S*-model.

The statistical parameters listed in Table 2 show that, in terms of conventional correlation (r^2) and cross-validation (q^2 and SDEP) coefficients, the model resulted statistically robust with values of 0.86, 0.70 and 0.54, respectively (*cross-validation 5 random groups* in GOLPE[60] program), while the *Leave One Out* validation method gave q^2 and SDEP values of 0.74 and 0.50, respectively.

Table 1
Inhibition of CYP19 and CYP17 by derivatives **1**–**4**

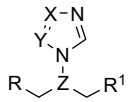

Compound	R	R^1	X	Y	Z	CYP19[a] IC_{50}[c] (μM) or % inhib. (36 μM)	CYP17[b] % inhib. (2.0 μM)
1ad	1-Naphthyl	4-*tert*-Butylphenyl	CH	CH	N	4.59	13
1an	1-Naphthyl	2,4-Dichlorophenyl	CH	CH	N	4.00	11.35
1bd	4-4′-Biphenyl	4-*tert*-Butylphenyl	CH	CH	N	2.16	NA[d]
1be	4-4′-Biphenyl	Phenyl	CH	CH	N	1.20	NA
1bf	4-4′-Biphenyl	2-Tolyl	CH	CH	N	2.96	20.57
1bg	4-4′-Biphenyl	2-Chlorophenyl	CH	CH	N	0.30	29.43
1bh	4-4′-Biphenyl	2-Fluorophenyl	CH	CH	N	0.46	NA
1bi	4-4′-Biphenyl	4-Tolyl	CH	CH	N	2.2	29.07
1bj	4-4′-Biphenyl	4-Chlorophenyl	CH	CH	N	1.18	13.57
1bk	4-4′-Biphenyl	4-Fluorophenyl	CH	CH	N	0.19	13.90
1bl	4-4′-Biphenyl	2-Methoxyphenyl	CH	CH	N	1.51	42.87
1bm	4-4′-Biphenyl	4-Methoxyphenyl	CH	CH	N	1.53	21.67
1bn	4-4′-Biphenyl	2,4-Dichlorophenyl	CH	CH	N	3.65	25.75
1bo	4-4′-Biphenyl	2,4-Difluorophenyl	CH	CH	N	0.35	NA
1dn	4-*tert*-Butylphenyl	2,4-Dichlorophenyl	CH	CH	N	1.52	43.30
1dp	4-*tert*-Butylphenyl	2-Thienyl	CH	CH	N	0.58	10.70
2bd	4-4′-Biphenyl	4-*tert*-Butylphenyl	CH	CH	CH	1.00	NA
2be	4-4′-Biphenyl	Phenyl	CH	CH	CH	0.95	17.10
2bf	4-4′-Biphenyl	2-Tolyl	CH	CH	CH	1.04	25.00
2bg	4-4′-Biphenyl	2-Chlorophenyl	CH	CH	CH	1.09	22.55
2bh	4-4′-Biphenyl	2-Fluorophenyl	CH	CH	CH	1.37	NA
2bi	4-4′-Biphenyl	4-Tolyl	CH	CH	CH	1.32	32.80
2bk	4-4′-Biphenyl	4-Fluorophenyl	CH	CH	CH	0.11	15.83
2bl	4-4′-Biphenyl	2-Methoxyphenyl	CH	CH	CH	0.51	30.20
2bm	4-4′-Biphenyl	4-Methoxyphenyl	CH	CH	CH	1.68	38.80
2bn	4-4′-Biphenyl	2,4-Dichlorophenyl	CH	CH	CH	1.24	18.23
2bo	4-4′-Biphenyl	2,4-Difluorophenyl	CH	CH	CH	0.26	17.70
3ac	1-Naphthyl	Cinnamyl	N	CH	N	(14.8%)	6.10
3ad	1-Naphthyl	4-*tert*-Butylphenyl	N	CH	N	NA	22.37
3an	1-Naphthyl	2,4-Dichlorophenyl	N	CH	N	(8.8%)	4.43
3bc	4-4′-Biphenyl	Cinnamyl	N	CH	N	(5.9%)	16.10
3bd	4-4′-Biphenyl	4-*tert*-Butylphenyl	N	CH	N	(8.8%)	15.95
3bn	4-4′-Biphenyl	2,4-Dichlorophenyl	N	CH	N	NA	13.05
3cn	Cinnamyl	2,4-Dichlorophenyl	N	CH	N	(10.6%)	NA
3dc	4-*tert*-Butylphenyl	Cinnamyl	N	CH	N	(38.3%)	19.93
3dn	4-*tert*-Butylphenyl	2,4-Dichlorophenyl	N	CH	N	(3.3%)	4.00
3dp	4-*tert*-Butylphenyl	2-Thienyl	N	CH	N	(30.7%)	NA
4ac	1-Naphthyl	Cinnamyl	CH	N	N	13.04	15.47
4ad	1-Naphthyl	4-*tert*-Butylphenyl	CH	N	N	(14.6%)	3.13
4an	1-Naphthyl	2,4-Dichlorophenyl	CH	N	N	(24.95%)	NA
4bc	4-4′-Biphenyl	Cinnamyl	CH	N	N	(31.4%)	12.40
4bd	4-4′-Biphenyl	4-*tert*-Butylphenyl	CH	N	N	(19.8%)	6.03
4bn	4-4′-Biphenyl	2,4-Dichlorophenyl	CH	N	N	(27.6%)	9.20
4cn	Cinnamyl	2,4-Dichlorophenyl	CH	N	N	17.13	21.05
4dc	4-*tert*-Butylphenyl	Cinnamyl	CH	N	N	5.06	12.40
4dn	4-*tert*-Butylphenyl	2,4-Dichlorophenyl	CH	N	N	(36%)	3.33
4dp	4-*tert*-Butylphenyl	2-Thienyl	CH	N	N	9.23	NA
Fadrozole						0.05	

[a] Human aromatase, placental microsomes, and substrate [1β,2β-^{3}H]testosterone, 500 nM.
[b] Human CYP17 expressed in *E. coli*, substrate progesterone, 25 μM.
[c] The given values are mean values of at least three experiments. The deviations were within ±5%.
[d] NA, no activity detected.

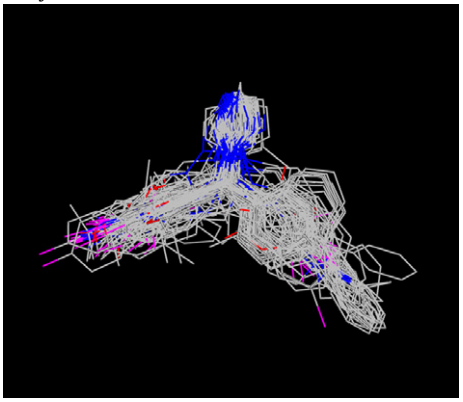

Figure 4. The 124 compounds of the training set as aligned by Surflex.

Besides the statistical evaluation, the assessment of its predictive ability is also an essential requirement for a 3D-QSAR model. Therefore with the aim to test the potential use of this model as an aid to design new aromatase inhibitors, an external data set (test set) of novel derivatives belonging to the series **1** and **2** (deriv-

Table 2
Statistical results of *R*-model with DRY+water (upper lines values) and DRY+OH (lower lines values) probes combination

q^2_{LOO}	$SDEP_{LOO}$	$q^2_{CV(5)}$	$r^2_{CV(5)}$	$SDEP_{CV(5)}$	Variables[a]	PCs[b]
0.66	0.58	0.64	0.82	0.60	1958	3
0.74	0.50	0.70	0.86	0.54	1475	3

[a] Number of GRID variables after the FFD selections.
[b] Number of principal components.

Table 3
Inhibition of CYP19 and CYP17 by derivatives **1bq**, **1eq**, **1nq**, **1er**, **1nr**, **2bq**, and **2eq**

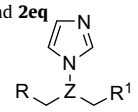

Compound	R	R^1	Z	CYP19[a] IC_{50}[c] (μM)	CYP17[b] % inhib. (2.0 μM)
1bq	4-4′-Biphenyl	5-Chloro-2-thienyl	N	1.04	23.60
1eq	Phenyl	5-Chloro-2-thienyl	N	1.06	7.30
1nq	2,4-Dichlorophenyl	5-Chloro-2-thienyl	N	0.32	56.20
1er	Phenyl	7-Benzothienyl	N	9.96	5.25
1nr	2,4-Dichlorophenyl	7-Benzothienyl	N	2.49	4.07
2bq	4-4′-Biphenyl	5-Chloro-2-thienyl	CH	1.07	25.70
2eq	Phenyl	5-Chloro-2-thienyl	CH	0.87	7.97

[a] Human aromatase, placental microsomes, and substrate [1β,2β-^{3}H]testosterone, 500 nM.
[b] Human CYP17 expressed in *E. coli*, substrate progesterone, 25 μM.
[c] The given values are mean values of at least three experiments. The deviations were within ±5%.

atives **1bq**, **1eq**, **1nq**, **1er**, **1nr**, **2bq**, and **2eq**, Fig. 3) was subjected to the 3D-QSAR model and then tested against CYP19 (and CYP17 as well) following the same protocols reported above. The results of the biological assays are reported in Table 3.

Indeed, although the pIC_{50} values of the newly synthesized molecules did not span over a wide range, their prediction was fairly good. The correlations between experimental and calculated/predicted pIC_{50} values (SDEP = 0.99) are shown in Figure 5.

Analysis of the GOLPE[60] PLS coefficients plots revealed that three areas (A, B, and C in Fig. 6) surrounding the ligand-based aligned molecules are important for the activity. In all the molecules of the training set the A region (green circle) is always occupied by substituents, thus highlighting the importance of this area in modulating the inhibitory potency. In fact, the large cyan-colored polyhedrons in this area are related to significant electrostatic and hydrogen bond interactions.

On the other side, the poor presence of large polyhedrons in the C region (blue circle) may suggest that this region is not significative for the activity. Nevertheless, most of the training set molecules are highly superimposed in this area, leading to low standard deviation on the grid points surrounding it. As a matter of fact, the PLS algorithm considers the regions corresponding to the missing polyhedrons as poorly correlating with the training set activities.

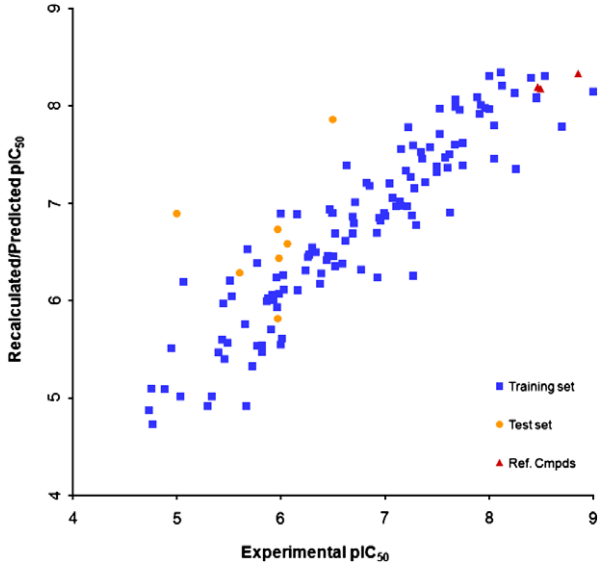

Figure 5. Experimental versus recalculated/predicted pIC_{50} plot. The molecules of the training set are indicated with blue squares while the compounds of the test set are indicated with orange circles. CGS-18320B, fadrozole, and vorozole were used as reference compounds and are indicated with deep red triangles.

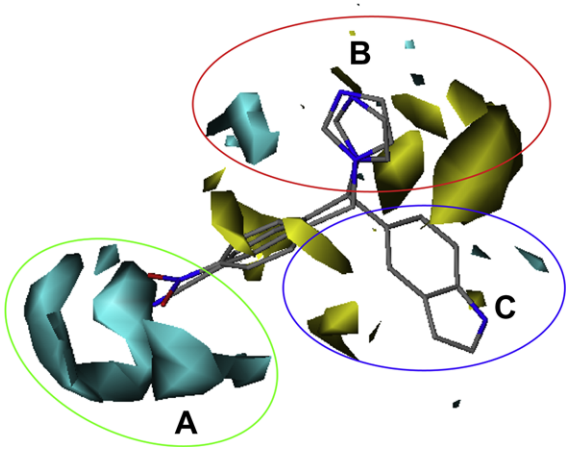

Figure 6. GRID plots of the PLS coefficients for the 3D-QSAR model. The cyan contours represent negative coefficients under −0.052 energy value while the yellow contours represent the positive coefficients over +0.0030. For a better visualization two active compounds (compound **15** of the **BMC1998** pool and compound **11R** of the **BMCL2006** pool; Supplementary data) are reported. For the sake of clarity hydrogen atoms are not displayed.

As regards to the B region (red circle), this is occupied by the azole moieties and is mainly described by positive PLS coefficients (yellow polyhedrons), in perfect agreement with the recognized importance of the coordination capability of such groups with the heme iron of the CYP enzyme.

The activity contribution plot, different for every molecule within the training set, gives the possibility to display spatial regions that are individually important for the selected molecules. In general, in the activity contribution plots cyan polyhedrons (negative values) show areas where a negative contribution to the inhibitory activity is associated, while yellow polyhedrons (positive values) indicate areas of positive contribution to the aromatase inhibitory activity.

This is more clearly explained in Figure 7, reporting the activity contribution plots relative to derivatives **2bk**, **2bh,** and **2bm**, respectively, the most and two of the least active among the compounds of the series **2** (Table 1). The decrease of activity from **2bk** (4-fluorophenyl-substituted) to **2bm** (4-methoxy-phenyl-substituted) could be ascribed to the higher sterical hindrance exerted by the methoxy group as showed by the cyan polyhedron close to the methyl group (central panel of Fig. 7). On the other hand, the lower activity of **2bh** if compared to **2bk** could be attributed

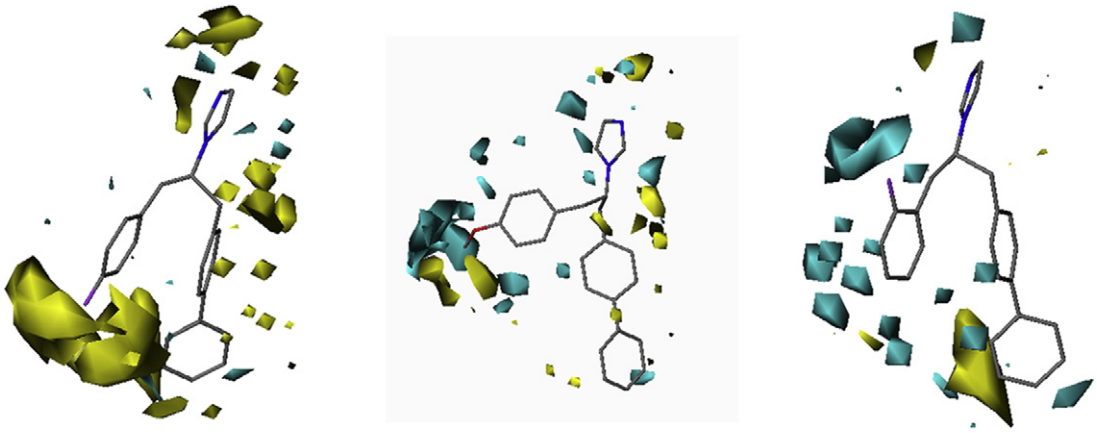

Figure 7. Activity contribution plots of the PLS coefficients for derivatives **2bk** (left), **2bm** (center), and **2bh** (right). The conformations of the three compounds are displayed as atom type colors. The cyan contours represent negative activity contribution areas while the yellow contours represent the positive activity contribution areas. For the sake of clarity hydrogen atoms are not displayed.

Table 4
Mulliken charges calculated with the program GAMESS

Compound	Substituent in position 4	Mulliken charge
1bi	Cl	0.038931
1bk	F	−0.409229
1bm	OMe	−0.715180
2bk	F	−0.411690
2bm	OMe	−0.820991

to the establishment by the 2-F substituent of unfavorable interactions (cyan polyhedrons in right panel of Fig. 7), that instead are missing in the case of the 4-F group (left panel of Fig. 7).

The difference in activity induced by the substituents (fluorine, chlorine, or methoxy) in the *para*-position could be explained by a combination of both sterical and electronic factors. In fact, ab initio calculations performed for the derivatives **1bj**, **1bk**, **1bm**, **2bk,** and **2bh** at the MP2/3-21G* level using the quantum chemistry program GAMESS[61] revealed that the negative charge on the fluorine atoms (compounds **1bk** and **2bk**, Table 4) is sufficient to account for a charge–charge bond or even for accepting a weak hydrogen bond. On the contrary, this interaction is not allowed for both the chlorine atom, positively charged and much bigger than fluorine (compare activity values of **1bj** and **1bk** in Table 1), and the methoxy substituent, negatively charged but whose free rotation could hinder the formation of the favorable interactions (compare activity values of **1bm** and **2bm** in Table 1 with those of **1bk** and **2bk**, respectively). Such scenario is fully in agreement with the activity contribution plots reported in Figure 7.

3. Conclusion

With the aim to investigate the potential of their common flexible backbone as a template for developing novel and selective aromatase inhibitors, we have tested the inhibitory activity against CYP19 and CYP17 of a library of antifungal agents previously reported by us. Indeed, even if lacking H-bond accepting substituents as CN or NO_2, several among the tested derivatives exhibited a good inhibitory potency against aromatase as well as a fairly good selectivity toward CYP17. However when we decided to build a 3D-QSAR model to rationalize and better understand the structure–activity relationships of such scaffold we realized the inadequacy to this purpose of a structure-based approach using previously described models. Therefore we turned to a ligand-based approach and after pooling the structures of 124 previously reported aromatase inhibitors into a structural-diversity-rich training set, we took advantage of the Surflex program and of the GRID/GOLPE procedure to develop a novel 3D-QSAR model, characterized by high robustness and self-consistency as substantiated by the high statistical coefficients. The analysis of the PLS coefficients plots revealed three regions crucial for the interaction of the inhibitors with the CYP enzyme and this fact, together with the capability to predict the activity of an external data set, propose this model as a helpful tool to design new aromatase inhibitors.

4. Experimental

4.1. Chemistry

4.1.1. General

All chemicals were purchased from Aldrich Chimica (Milan, Italy) or from Lancaster Synthesis GmbH (Milan, Italy) and were of the highest purity. All solvents were reagent grade and, when necessary, were purified and dried by standard methods. Reactions were routinely monitored by TLC performed on aluminum-backed silica gel plates (Merck DC, Alufolien Kieselgel 60 F_{254}) with spots visualized by UV light (λ = 254 and 365 nm) or using a $KMnO_4$ alkaline solution. Concentration of solutions after reactions and extractions involved the use of a rotary evaporator operating at a reduced pressure of ~10 Torr. Organic solutions were dried over anhydrous sodium sulfate. Chromatographic separations were performed on silica gel (Silica gel 60, 0.063–0.200 mm; Merck DC) or on alumina (aluminium oxide 90, active, neutral, 0.063–0.200 mm; Merck DC) columns. Melting points were determined on a Gallenkamp melting point apparatus in open capillary tubes and are uncorrected. Infrared (IR) spectra (KBr) were recorded on a Shimadzu FTIR-8000 instrument. ^{1}H NMR spectra were recorded at 300 MHz on a Bruker Avance 300 spectrometer; chemical shifts are reported in δ (ppm) units relative to the internal reference tetramethylsilane (Me_4Si). Mass spectra were recorded on a Finnigan LCQ DECA TermoQuest (San Jose, CA) mass spectrometer using an electrospray ion source (ESI-MS). The elemental compositions of the compounds agreed to within ±0.4% of the calculated value. When the elemental analysis is not included, crude compounds were used in the next step without further purification. As a rule, samples prepared for physical and biological studies were dried in high vacuum over P_2O_5 for 20 h at temperatures ranging from 25 to 110 °C, depending on the sample melting point. The Schiff bases **5b**, **5e,** and **5n**,[34] the corresponding secondary amines **6b**, **6e,** and **6n**,[34] the imidazolylacetophenones **7b**[48] and **7e,**[49] as well as 7-(bromomethyl)benzothiophene[47] were prepared according to procedures described in the literature.

4.1.2. Synthesis of 3-(5-chlorothiophen-2-yl)-2-(1*H*-imidazol-1-yl)-1-phenylpropan-1-one (8eq)

To a stirred suspension of NaH (0.576 g, 24 mmol) in dry THF (20 ml) a solution of 2-(1-imidazolyl)acetophenone **7e**[49] (3.72 g, 20 mmol) in dry THF was added. After stirring at room temperature for 1 h, a solution of 2-chloro-5-(chloromethyl)thiophene (3.34 g, 20 mmol) in dry THF (20 mL) was added dropwise and the reaction was kept stirring at 50 °C for 3 h. The reaction mixture was then cooled to room temperature, quenched with methanol (2.0 mL) and concentrated under vacuum. The crude product was partitioned between diethyl ether (100 mL) and water (100 mL) and the aqueous layer was separated and extracted with diethyl ether (3× 50 mL). The combined organic layers were washed with brine, then dried over Na_2SO_4 and concentrated. The resulting crude material was purified by column chromatography on silica gel eluting with AcOEt to yield pure **8eq** (2.28 g, 36%) as a colorless glass-like solid which was crystallized as an oxalate salt from ethanol/diethyl ether (mp 176–178 °C). ^{1}H NMR ($CDCl_3$): δ 7.93–7.82 (m, 2H), 7.65–7.40 (m, 4H), 7.04 (s, 1H), 6.99 (s, 1H), 6.64 (d, 1H, J = 3.8 Hz), 6.36 (d, 1H, J = 3.8 Hz), 5.70 (dd, 1H, J = 8.8, 5.1 Hz), 3.55 (dd, 1H, J = 15.4, 5.1 Hz), 3.35 (dd, 1H, J = 15.4, 8.8 Hz). ESI-MS *m/z*: 317 (M+H). IR (KBr) 1697 (C=O) cm^{-1}. Anal. Calcd for $C_{16}H_{13}ClN_2OS\cdot C_2H_2O_4$: C, 53.14; H, 3.72; N, 6.89. Found: C, 53.25; H, 3.72; N, 6.88.

4.1.3. Synthesis of 1-[1,1′-biphenyl]-4-yl-3-(5-chlorothio-phen-2-yl)-2-(1*H*-imidazol-1-yl)propan-1-one (8bq)

The alkylation of the imidazolylacetophenone **7b**[48] according to the same procedure described above yielded pure **8bq** (34%) as a white solid (mp 142–143 °C). ^{1}H NMR ($CDCl_3$): δ 7.96 (d, 2H, J = 7.9 Hz), 7.70–7.30 (m, 8H), 7.08 (s, 1H), 7.03 (s, 1H), 6.68 (d, 1H, J = 3.9 Hz), 6.40 (d, 1H, J = 3.9 Hz), 5.73 (dd, 1H, J = 8.9, 5.3 Hz), 3.55 (dd, 1H, J = 15.2, 5.3 Hz), 3.35 (dd, 1H, J = 15.2, 8.9 Hz). ESI-MS *m/z*: 393 (M+H). IR (KBr) 1681 (C=O) cm^{-1}. Anal. Calcd for $C_{22}H_{17}ClN_2OS$: C, 67.25; H, 4.36; N, 7.13. Found: C, 67.38; H, 4.35; N, 7.12.

4.1.4. Synthesis of 1-(5-chlorothiophen-2-yl)-2-(1*H*-imidazol-1-yl)-3-phenylpropane (2eq)

A mixture of 3-(5-chlorothiophen-2-yl)-2-(1*H*-imidazol-1-yl)-1-phenylpropan-1-one **8eq** (1.78 g, 5.64 mmol), hydrazine monohydrate (1.37 mL, 28.2 mmol), ethylene glycol (50 mL) and potassium hydroxide (2.59 g, 46.2 mmol) was heated at 185–190 °C for 3 h. The reaction mixture was then cooled to room temperature, poured into 500 mL of water, acidified to pH ≈ 1.0 with concentrated hydrochloric acid and extracted with chloroform (3× 50 mL). The organic extract was washed with brine, dried over Na_2SO_4 and concentrated. The crude product was purified by column chromatography on silica gel eluting with AcOEt to yield pure **2eq** (0.46 g, 27%) as a colorless glass-like solid which was crystallized as an oxalate salt from ethanol/diethyl ether (mp 182–184 °C). ^{1}H NMR ($CDCl_3$): δ 7.36–6.80 (m, 8H), 6.63 (d, 1H, J = 3.1 Hz), 6.34 (d, 1H, J = 3.1 Hz), 4.40–4.19 (m, 1H), 3.34–2.95 (m, 4H). ESI-MS *m/z*: 303 (M+H). Anal. Calcd for $C_{16}H_{15}ClN_2S\cdot C_2H_2O_4$: C, 55.03; H, 4.36; N, 7.13. Found: C, 55.15; H, 4.36; N, 7.11.

4.1.5. Synthesis of 1-(1,1′-biphenyl-4-yl)-3-(5-chloro-thiophen-2-yl)-2-(1*H*-imidazol-1-yl)propane (2bq)

Following the same procedure described above, title derivative **2bq** was obtained starting from **8bq** as a pure colorless glass-like solid (yield: 34%) which was crystallized as an oxalate salt from ethanol/diethyl ether (mp 143–144 °C). ^{1}H NMR ($CDCl_3$): δ 7.40–6.78 (m, 12H), 6.65 (d, 1H, J = 3.2 Hz), 6.40 (d, 1H, J = 3.2 Hz), 4.42–4.18 (m, 1H), 3.36–2.98 (m, 4H). ESI-MS *m/z*: 379 (M+H). Anal. Calcd for $C_{22}H_{19}ClN_2S\cdot C_2H_2O_4$: C, 61.47; H, 4.51; N, 5.97. Found: C, 61.60; H, 4.52; N, 5.96.

4.1.6. Synthesis of *N*-benzyl-*N*-(5-chlorothiophen-2-yl-methyl)-1*H*-imidazol-1-amine (1eq)

A solution of *N*-benzyl-1*H*-imidazol-1-amine **6e**[34] (1.73 g, 10.0 mmol) and tetrabutylammonium hydrogen sulfate (3.39 g, 10.0 mmol) in DCM (50 mL) was treated with 2-chloro-5-(chloromethyl)thiophene (2.51 g, 15.0 mmol) and 50% sodium hydroxide aqueous solution (30 mL). After stirring at room temperature for 15 h, DCM (60 mL) was added and the mixture was poured into ice-water (60 mL). The aqueous layer was separated and extracted with DCM (3× 50 mL). Combined organic layers were washed with brine, dried over Na_2SO_4 and concentrated. The resulting crude material was purified by column chromatography on silica gel eluting with AcOEt to yield pure **1eq** (1.00 g, 33%) as a colorless glass-like solid which was crystallized as an oxalate salt from ethanol/diethyl ether (mp 147 °C). ^{1}H NMR ($CDCl_3$): δ 7.30–7.17 (m, 6H), 7.10–7.03 (m, 1H), 6.95–6.88 (m, 1H), 6.65 (d, 1H, J = 1.8 Hz), 6.53 (d, 1H, J = 1.8 Hz), 4.24 (s, 2H), 4.15 (s, 2H). ESI-MS *m/z*: 304 (M+H). Anal. Calcd for $C_{15}H_{14}ClN_3S\cdot C_2H_2O_4$: C, 51.84; H, 4.09; N, 10.67. Found: C, 51.96; H, 4.10; N, 10.64.

4.1.7. Synthesis of *N*-benzyl-*N*-(benzo[b]thiophen-7-ylmethyl)-1*H*-imidazol-1-amine (1er)

A mixture of *N*-benzyl-1*H*-imidazol-1-amine **6e**[34] (1.73 g, 10.0 mmol), potassium *tert*-butoxide (1.12 g, 10.0 mmol) and 18-crown-6 (0.27 g, 1.00 mmol) in diethylether (20 mL) was stirred at room temperature under nitrogen for 15 min. The reaction mixture was cooled to 0 °C and a solution of 7-(bromomethyl)benzothiophene[47] (1.99 g, 10.0 mmol) in diethylether (10 mL) was added dropwise. The mixture was stirred at room temperature for 4 h and then poured into water (60 mL). The aqueous layer was separated and extracted with AcOEt (3× 50 mL). The combined organic phases were washed with brine, dried over Na_2SO_4 and concentrated. The resulting crude material was purified by column chromatography on silica gel eluting with AcOEt to yield pure **1er** (1.15 g, 36%) as a colorless glass-like solid which was crystallized from benzene/ligroin (mp 110–112 °C). ^{1}H NMR ($CDCl_3$): δ 7.78–7.69 (m, 1H), 7.52–7.08 (m, 11H), 6.91–6.86 (m, 1H), 4.45 (s, 2H), 4.17 (s, 2H). ESI-MS *m/z*: 320 (M+H). Anal. Calcd for $C_{19}H_{17}N_3S$: C, 71.44; H, 5.36; N, 13.15. Found: C, 71.60; H, 5.37; N, 13.13.

4.1.8. Synthesis of *N*-(1,1′-biphenyl-4-ylmethyl)-*N*-(5-chlorothiophen-2-ylmethyl)-1*H*-imidazol-1-amine (1bq)

The alkylation of *N*-[(1,1′-biphenyl)-4-ylmethyl]-1*H*-imidazol-1-amine **6b**[34] with 2-chloro-5-(chloromethyl)thio-phene following the same procedure described for **1eq**, yielded pure **1bq** (81%) as a colorless glass-like solid which was crystallized as a hydrochloride salt from ethanol/diethyl ether (mp 169–171 °C). ^{1}H NMR ($CDCl_3$): δ *7.60–7.25* (m, 10H), 7.13 (s, 1H), 6.98 (s, 1H), 6.69 (d, 1H, J = 3.7 Hz), 6.57 (d, 1H, J = 3.7 Hz), 4.29 (s, 2H), 4.27 (s, 2H). ESI-MS *m/z*: 380 (M+H). Anal. Calcd for $C_{19}H_{18}ClN_3S\cdot HCl$: C, 60.58; H, 4.60; N, 10.09. Found: C, 60.69; H, 4.60; N, 10.07.

4.1.9. Synthesis of *N*-(5-chlorothiophen-2-ylmethyl)-*N*-(2,4-dichlorobenzyl)-1*H*-imidazol-1-amine (1nq)

The alkylation of *N*-(2,4-dichlorobenzyl)-1*H*-imidazol-1-amine **6n**[34] with 2-chloro-5-(chloromethyl)thiophene following the same procedure described for **1eq**, yielded pure **1nq** (32%) as a white glass-like solid which was crystallized from benzene/ligroin (mp 106 °C). ^{1}H NMR ($CDCl_3$): δ 7.38–7.33 (m, 1H), 7.25–7.22 (m, 1H), 7.14–7.08 (m, 3H), 6.98–6.91 (m, 1H), 6.65 (d, 1H, J = 3.8 Hz), 6.55 (d, 1H, J = 3.8 Hz),4.29 (s, 2H), 4.27 (s, 2H). ESI-MS *m/z*: 374 (M+H). Anal. Calcd for $C_{15}H_{12}Cl_3N_3S$: C, 48.34; H, 3.25; N, 11.27. Found: C, 48.44; H, 3.26; N, 11.24.

4.1.10. Synthesis of *N*-(benzo[b]thiophen-7-ylmethyl)-*N*-(2,4-dichlorobenzyl)-1*H*-imidazol-1-amine (1nr)

The alkylation of *N*-(2,4-dichlorobenzyl)-1*H*-imidazol-1-amine **6n**[34] with 7-(bromomethyl)benzothiophene[47] following the procedure described for **1eq**, yielded pure **1nr** (26%) as a white glass-like solid which was crystallized as an oxalate salt from ethanol/diethyl ether (mp 145–147 °C). ^{1}H NMR ($CDCl_3$): δ *7.77–7.68* (m, 1H), 7.51–7.08 (m, 9H), 6.93–6.84 (m, 1H), 4.49 (s, 2H), 4.31 (s, 2H). ESI-MS *m/z*: 388 (M+H). Anal. Calcd for $C_{19}H_{15}Cl_2N_3S{\cdot}C_2H_2O_4$: C, 52.73; H, 3.58; N, 8.78. Found: C, 52.84; H, 3.59; N, 8.76.

4.2. Biology

4.2.1. CYP19 preparation and assay

The microsomal fraction of freshly delivered human term placenta provided the source of the aromatase enzyme. The compounds were tested for aromatase inhibitory activity[62] using the ^3H_2O-method introduced by Thompson and Siiteri.[44] [1β, 2β-^{3}H]testosterone was used as substrate.

4.2.2. CYP17 preparation and assay

Human CYP17 was obtained from *E. coli* coexpressing human CYP17 and NADPH-P450 reductase[63] by homogenization and fractional centrifugation.[45] The assay was performed using the 50,000*g* sediment and progesterone as substrate as described.[45]

4.3. Molecular modeling

All the tested molecules were built, starting from ASCII text, using the standalone version of PRODRG[51–53] in conjunction with GROMACS suite.[64] The alignment of the compounds was achieved by means of the Surflex program,[55] using the crystal structures of CGS-18320B,[56] fadrozole,[56] and vorozole[57] as reference molecules, previously rigidly aligned with the program Surflex. The Chimera 1.2176 program[65] was used to produce the images on a 3GHz AMD CPU equipped IBM compatible workstation with the SUSE 9.0 version of the Linux operating system.

The training set of 124 molecules was obtained by pooling 31 compounds belonging to the **1–2** and **4** series,[50] the three reference compounds (vorozole, anastrozole, and fadrozole), and 90 previously reported aromatase inhibitors (Fig. 4).[20–22,40–43,51]

4.3.1. GRID calculations

The interaction energies were calculated by using the program GRID[66] (version 22) with a grid spacing of 1 Å and the grid dimensions (Å): X_{min}/X_{max}, −8.0/20.0; Y_{min}/Y_{max}, −13.0/13.0; and Z_{min}/Z_{max}, −13.0/13.0.

4.3.2. GOLPE analyses

PLS models were calculated with GOLPE 4.5.12[67] running on a SGI O2 R10000 equipped with the IRIX operating system 6.5.11. To measure the goodness of the model the statistical indices r^2, q^2 and SDEP were employed.

4.3.3. Ab initio calculations

Partial atomic charges on the substituents in the *para*-position of compounds **1bj**, **1bk**, **1bm**, **2bk,** and **2bh** of the training set were calculated by using the GAMESS package[61] and the MP2/3-21G* basis set.

Acknowledgments

Many thanks are due to Prof. Gabriele Cruciani and Prof. Sergio Clementi (Molecular Discovery and MIA srl) for the use the GOLPE program in their chemometric laboratory (University of Perugia, Italy) and for having provided the GRID program. This work was partially supported by grants from Regione Campania 2003, LR 5/02, Ministero dell'Università e della Ricerca Scientifica e Tecnologica (PRIN 2005), and Università di Salerno, Italy (G.S.). Thanks are due to Martina Jankowski for the help performing the enzyme assays.

Supplementary data

Supplementary data associated with this article can be found, in the online version, at doi:10.1016/j.bmc.2008.08.046.

References and notes

1. American Cancer Society web site. http://www.cancer.org and http://www.imaginis.com.
2. Chen, S.; Zhou, D.; Okubo, T.; Kao, Y. C.; Eng, E. T.; Grube, B.; Kwon, A.; Yang, C.; Yu, B. *Ann. N. Y. Acad. Sci.* **2002**, *963*, 229.
3. Geisler, H. *J. Steroid Biochem. Mol. Biol.* **2003**, *86*, 245.
4. Bruno, R. D.; Njar, V. C. O. *Bioorg. Med. Chem.* **2007**, *15*, 5047.
5. Brueggemeier, R. W.; Hackett, J. C.; Diaz-Cruz, E. S. *Endocr. Rev.* **2005**, *26*, 331.
6. Brodie, A.; Brodie, H. B.; Callard, G.; Robinson, C.; Roselli, C.; Santen, R. *J. Steroid Biochem. Mol. Biol.* **1993**, *44*, 321.
7. Foster, A. B.; Jarman, M.; Leung, C. S.; Rowlands, M. G.; Taylor, G. N.; Plevey, R. G.; Sampson, P. *J. Med. Chem.* **1985**, *28*, 200.
8. Daly, M. J.; Jones, G. W.; Nicholls, P. J.; Smith, H. J.; Rowlands, M. G.; Bunnett, M. A. *J. Med. Chem.* **1986**, *29*, 520.
9. Hartmann, R. W.; Batzl, C.; Pongratz, T. M.; Mannschreck, A. *J. Med. Chem.* **1992**, *35*, 2210.
10. Bossche, H. V. *J. Steroid Biochem. Mol. Biol.* **1992**, *43*, 1003.
11. Karjalainen, A.; Kalapudas, A.; Södervall, M.; Pelkonen, O.; Lammintausta, R. *Eur. J. Pharm. Sci.* **2000**, *11*, 109.
12. Attar, E.; Bulun, S. E. *Fertil. Steril.* **2006**, *85*, 1307.
13. Geisler, J.; Lonning, E. *Clin. Cancer Res.* **2005**, *11*, 2809.
14. Michaud, L. B. *Am. J. Health-Syst. Pharm.* **2005**, *62*, 266.
15. Miller, W. R. *Semin. Oncol.* **2003**, *30*, 3.
16. Recanatini, M.; Cavalli, A.; Valenti, P. *Med. Res. Rev.* **2002**, *22*, 282. and references therein reported.
17. Kelloff, G. J.; Lubet, R. A.; Lieberman, R.; Eisenhauer, K.; Steele, V. E.; Crowell, J. A.; Hawk, E. T.; Boone, C. W.; Sigman, C. C. *Cancer Epidemiol. Biomarkers Prev.* **1998**, *7*, 65.
18. Saberi, M. R.; Vinh, T. K.; Yee, S. W.; Griffiths, B. J. N.; Evans, P. J.; Simons, C. *J. Med. Chem.* **2006**, *49*, 1016.
19. Su, B.; Diaz-Cruz, E. S.; Landini, S.; Brueggemeier, R. W. *J. Med. Chem.* **2006**, *49*, 1413.
20. Lézé, M. P.; Le Borgne, M.; Pinson, P.; Palusczak, A.; Duflos, M.; Le Baut, G.; Hartmann, R. W. *Bioorg. Med. Chem. Lett.* **2006**, *16*, 1134.
21. Recanatini, M.; Bisi, A.; Cavalli, A.; Belluti, F.; Gobbi, S.; Rampa, A.; Valenti, P.; Palzer, M.; Palusczak, A.; Hartmann, R. W. *J. Med. Chem.* **2001**, *44*, 672.
22. Cavalli, A.; Bisi, A.; Bertucci, C.; Rosini, C.; Paluszcak, A.; Gobbi, S.; Giorgio, E.; Rampa, A.; Belluti, F.; Piazzi, L.; Valenti, P.; Hartmann, R. W.; Recanatini, M. *J. Med. Chem.* **2005**, *48*, 7282.
23. Gobbi, S.; Cavalli, A.; Rampa, A.; Belluti, F.; Piazzi, L.; Paluszcak, A.; Hartmann, R. W.; Recanatini, M.; Bisi, A. *J. Med. Chem.* **2006**, *49*, 4777.
24. Gobbi, S.; Cavalli, A.; Negri, M.; Schewe, K. E.; Belluti, F.; Piazzi, L.; Hartmann, R. W.; Recanatini, M.; Bisi, A. *J. Med. Chem.* **2007**, *50*, 3420.
25. Okada, M.; Yoden, T.; Kawaminami, E.; Shimada, Y.; Kudoh, M.; Isomura, Y.; Shikama, H.; Fujikura, T. *Chem. Pharm. Bull.* **1996**, *44*, 1871.
26. Howell, A.; Robertson, J. F. R.; Vergote, I. A. *Breast Cancer Res.* **2003**, *82*, 215.
27. Scott, J. L.; Keam, J. S. *Drugs* **2006**, *66*, 353.
28. Lonning, P. E.; Bajetta, E.; Murray, R.; Tubiana-Hulin, M.; Eisenberg, P. D.; Mickiewicz, E.; Celio, L.; Pitt, P.; Mita, M.; Aaronson, N. K.; Fowst, C.; Arkhipov, A.; di Salle, E.; Polli, A.; Massimini, G. *J. Clin. Oncol.* **2000**, *18*, 2234.
29. Thurlimann, B.; Keshaviah, A.; Coates, A. S.; Mouridsen, H.; Mauriac, L.; Forbes, J. F.; Paridaens, M.; Castiglione-Gertsch, M.; Gelber, R. D.; Rabaglio, M.; Smith, I.; Wardley, A.; Price, K. N.; Goldhirsch, A. N. *Engl. J. Med.* **2005**, *353*, 2747.
30. Jakesz, R.; Jonet, W.; Gnant, M.; Mittleboeck, M.; Greil, R.; Tausch, C.; Hilfrich, J.; Kwasny, W.; Menzel, C.; Samonigg, H. *Lancet* **2005**, *366*, 455.
31. Osborne, C.; Tripathy, D. *Annu. Rev. Med.* **2005**, *56*, 103.
32. Jackson, J.; Miller, W. R.; Dixon, J. M. *Expert Opin. Drug Saf.* **2003**, *2*, 73.
33. Castellano, S.; La Colla, P.; Musiu, C.; Stefancich, G. *Arch. Pharm. (Weinheim, Ger.)* **2000**, *333*, 162.
34. Castellano, S.; Stefancich, G.; Musiu, C.; La Colla, P. *Arch. Pharm. (Weinheim, Ger.)* **2000**, *333*, 299.
35. Setzu, M. G.; Stefancich, G.; La Colla, P.; Castellano, S. *Farmaco* **2002**, *57*, 1015.
36. Castellano, S.; Stefancich, G.; Chillotti, A.; Poni, G. *Farmaco* **2003**, *58*, 563.
37. Furet, P.; Batzl, C.; Bhatnagar, A.; Francotte, E.; Rihs, G.; Lang, M. *J. Med. Chem.* **1993**, *36*, 1393.
38. Koymans, L. M. H.; Moereels, H.; Bossche, H. V. *J. Steroid Biochem. Mol. Biol.* **1995**, *53*, 191.
39. Jackson, T.; Lawrence Woo, L. W.; Trusselle, M. N.; Purohit, A.; Reed, M. J.; Potter, B. V. L. *ChemMedChem* **2008**, *3*, 603.

40. Le Borgne, M.; Marchand, P.; Duflos, M.; Delevoye-Seiller, B.; Piessard-Robert, S.; Le Baut, G.; Hartmann, R. W.; Palzer, M. *Arch. Pharm. (Weinheim, Ger.)* **1997**, *330*, 141.
41. Le Borgne, M.; Marchand, P.; Delevoye-Seiller, B.; Robert, J. M.; Le Baut, G.; Hartmann, R. W.; Palzer, M. *Bioorg. Med. Chem. Lett.* **1999**, *9*, 333.
42. Marchand, P.; Le Borgne, M.; Palzer, M.; Le Baut, G.; Hartmann, R. W. *Bioorg. Med. Chem. Lett.* **2003**, *13*, 1553.
43. Hartmann, R. W.; Palusczak, A.; Lacan, F.; Ricci, G.; Ruzziconi, R. *J. Enzyme Inhib. Med. Chem.* **2004**, *19*, 145.
44. Thompson, E. A., Jr.; Siiteri, P. K. *J. Biol. Chem.* **1974**, *249*, 5364.
45. Hutschenreuter, T. U.; Ehmer, P. B.; Hartmann, R. W. *J. Enzyme Inhib. Med. Chem.* **2004**, *19*, 17.
46. Hartmann, R. W.; Bayer, H.; Gruen, G.; Sergejew, T.; Bartz, U.; Mitrenga, M. *J. Med. Chem.* **1995**, *38*, 2103.
47. Nussbaumer, P.; Petranyi, G.; Stuetz, A. *J. Med. Chem.* **1991**, *34*, 65.
48. Nardi, D.; Tajana, A.; Leonardi, A.; Pennini, R.; Portioli, F.; Magistretti, M. J.; Subissi, A. *J. Med. Chem.* **1981**, *24*, 727.
49. Baji, H.; Flammang, M.; Kimny, T.; Gasquez, F.; Compagnon, P. L.; Delcourt, A. *Eur. J. Med. Chem.* **1995**, *30*, 617.
50. The structures of derivatives of the series **3** and **4** (with the exception of compounds **4ac**, **4cn**, **4dc**, and **4dp**), for which just the percentages of inhibition and not IC_{50} values were reported in Table 1, were not included in the training set.
51. Recanatini, M.; Cavalli, A. *Bioorg. Med. Chem.* **1998**, *6*, 377.
52. For academic research purposes PRODRG2 is freely available as a WWW service at http://davapc1.bioch.dundee.ac.uk/prodrg/index.html.
53. Schuttelkopf, A. W.; van Aalten, D. M. *Acta Crystallogr., Sect. D Biol. Crystallogr.* **2004**, *60*, 1355.
54. van Aalten, D. M.; Bywater, R.; Findlay, J. B.; Hendlich, M.; Hooft, R. W.; Vriend, G. *J. Comput. Aided Mol. Des.* **1996**, *10*, 255.
55. Favia, A. D.; Cavalli, A.; Masetti, M.; Carotti, A.; Recanatini, M. *Proteins Struct. Funct., Bioinf.* **2006**, *62*, 1074.
56. Jain, A. N. *J. Med. Chem.* **2003**, *46*, 499.
57. Van Roey, P.; Bullion, K. A.; Osawa, Y.; Browne, L. J.; Bowman, R. M.; Braun, D. G. *J. Enzyme Inhib. Med. Chem.* **1991**, *5*, 119.
58. Peeters, O. M.; Schuerman, G. S.; Blaton, N. M.; De Ranter, C. J. *Acta Crystallogr., Sect. C Cryst. Struct. Commun.* **1958**, *1993*, 49.
59. Ragno, R.; Simeoni, S.; Valente, S.; Massa, S.; Mai, A. *J. Chem. Inf. Model.* **2006**, *46*, 1420.
60. Baroni, M.; Costantino, G.; Cruciani, G.; Riganelli, D.; Valigi, R.; Clementi, S. *Quant. Struct.-Act. Relat.* **1993**, *12*, 9.
61. Schmidt, M. W.; Baldridge, K. K.; Boatz, J. A.; Elbert, S. T.; Gordon, M. S.; Jensen, J. H.; Koseki, S.; Matsunaga, N.; Nguyen, K. A.; Su, S.; Windus, T. L.; Dupuis, M.; John, A.; Montgomery, J. *Comput. Chem.* **1993**, *14*, 1347.
62. Hartmann, R. W.; Batzl, C. *J. Med. Chem.* **1986**, *29*, 1362.
63. Ehmer, P. B.; Jose, J.; Hartmann, R. W. *J. Steroid Biochem. Mol. Biol.* **2000**, *75*, 57.
64. Van Der Spoel, D.; Lindahl, E.; Hess, B.; Groenhof, G.; Mark, A. E.; Berendsen, H. J. C. *J. Comput. Chem.* **2005**, *26*, 1701.
65. Pettersen, E. F.; Goddard, T. D.; Huang, C. C.; Couch, G. S.; Greenblatt, D. M.; Meng, E. C.; Ferrin, T. E. *J. Comput. Chem.* **2004**, *25*, 1605.
66. Goodford, P. J. *J. Med. Chem.* **1985**, *28*, 849.
67. GOLPE 4.5; Multivariate Infometric Analysis Srl.: Viale dei Castagni 16, Perugia, Italy, 1999.